Scalable Computing: Practice and Experience, ISSN 1895-1767, http://www.scpe.org
© 2024 SCPE. Volume 25, Issues 6, pp. 5416–5423, DOI 10.12694/scpe.v25i6.3417

AUTOMOBILE INTELLIGENT VEHICLE-MACHINE AND HUMAN-COMPUTER INTERACTION SYSTEM BASED ON BIG DATA

QUANYU WANG*AND YAO ZHANG†

Abstract. This paper measures the accelerator, brake pedal, clutch, transmission device and steering wheel under different driving conditions in real-time and accurately on the simulation experiment platform. The goal is to conduct human-machine-road system interaction in a virtual simulation of human-vehicle-road systems. Fitting test data establishes the mathematical model of traffic control parameters. In terms of hardware, the distributed architecture of upper and lower computers is utilized. The system communicates point-to-point with the host computer through the RS-232 serial port. The system adopts multi-thread technology and serial communication technology. The simulation system of driving operation is designed with the visual central controller. The system takes 89S52 as the core. The slave program is written in C language. Then, the system establishes a multi-target coordinated obstacle avoidance method based on a multi-sensor information vehicle cooperation collision avoidance method. The multi-vehicle cooperation obstacle avoidance problem is transformed into an optimal control problem under multiple constraints. Simulation analysis shows that the velocity and displacement obtained by the multi-robot collaborative collision avoidance method are in good agreement with the measured values. Compared with the time series algorithm, the output accuracy of the proposed collaborative collision avoidance algorithm is significantly reduced, and the changes in velocity and displacement in the time domain are more stable.

Key words: Virtual simulation; Man-car-road; Data acquisition; Smart car; Human-computer interaction; Vehicle collaborative collision avoidance control algorithm; Serial communication

1. Introduction. Human-vehicle-road virtual simulation is a comprehensive technology used in safety assessment and design optimization of highway alignment and traffic engineering facilities. This method constructs 3D modeling of roads, facilities and other virtual simulation experiments with high immersion. It transforms digital data into a visual simulation process that can change over time and space [1]. Various quantitative indicators can be obtained to scientifically evaluate the use effect and safety of roads to provide scientific reference for road design using human-vehicle-road virtual simulation technology [2]. Intersection is a common and complicated driving condition, which is restricted by many factors such as driving mode, vehicle type, traffic rules, etc. By building mathematical models, machine analysis enables researchers to understand the connections between their inputs and outputs more directly. However, due to its inability to cover a variety of factors, its prediction accuracy is not high. Under high speed and low adhesion road surface conditions, steering obstacle avoidance is better than braking obstacle avoidance. In the human-vehicle-road virtual simulation, the simulation device is required to complete the real-time control of the vehicle in the virtual environment [3]. Therefore, it is an essential technology for obtaining data on driving control signals in the virtual simulation of a human-vehicle road. At the same time, this paper studies the dynamic optimization method of vehicle cooperative lane change obstacle avoidance based on "mechanism + data."

2. Hardware development of driving data acquisition system.

2.1. System hardware design.

The virtual simulation of a human-vehicle road uses the driver's console as the input device. The experiment was performed on a three-channel cylindrical projection display. In terms of hardware, it adopts the distributed serial port of the upper computer and the lower computer [4]. Point-to-point communication is adopted. The PC uses an 89S52 microcontroller. The visual master computer is used as hardware. An embedded system is adopted. The architecture of the system is described in Figure 2.1. The system layout of the lower computer is shown in Figure 2.2. For the communication part of the slave machine,

*Department of Automotive Engineering, Hebi Automobile Engineering Professional College, Hebi Henan, 458000, China (Corresponding author, wqy920405@163.com)
†Department of Automotive Engineering, Hebi Automobile Engineering Professional College, Hebi Henan, 458000, China

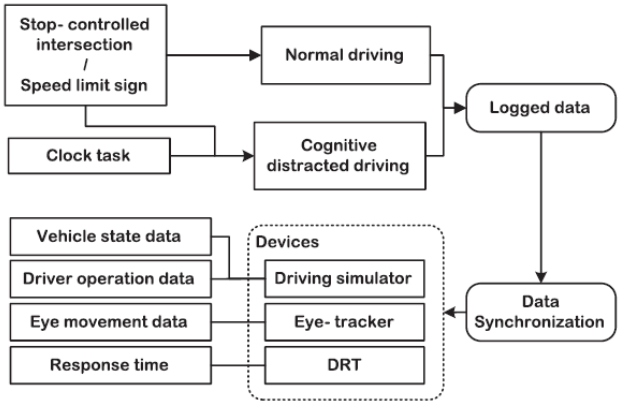

Fig. 2.1: . *Architecture of driving data acquisition system.*

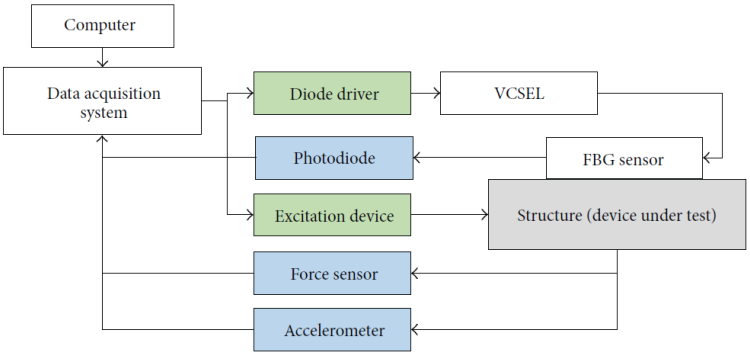

Fig. 2.2: *Layout of the driving data acquisition system.*

MAX202 from the German Maxim company was selected. In this way, the TTL level is converted to RS-232. This paper introduces an intelligent measurement system based on 89S52 microcontroller [5]. It has 8KB of flash memory and does not require memory expansion. The device uses 32 KB RAM as a data storage area and is also used for signal acquisition.

The angle of the steering wheel and the displacement of the accelerator pedal, brake pedal, and clutch pedal are measured by a high-precision potentiometer on a simulated driving test platform [6]. The excitation voltage of the sensor in the system is 10 V, provided by an analog signal regulation circuit. The transducer's output signal is amplified, transformed and converted into a reference voltage of 0-10 V. Then it is sent to the analog-to-digital converter to complete the A/D conversion. The shift lever only changes suddenly at a particular moment during the shift and is constant most of the time. Six switches on the shift lever indicate the condition of the 1, 2, 3, 4, 5 and R gears, respectively. It is driven and adjusted by the photoelectric separation's switching input signal regulation module.

2.2. Software Design.

2.2.1. Communication Protocol. It is necessary to communicate reasonably to ensure reliable communication between the upper and lower computers [7]. The definition of communication mode is shown in Table 2.1. A formal description of the command framework is given in Table 2.2. The format description of the data frame is given in Table 2.3. A formal description of the data areas is listed in Table 2.4.

Table 2.1: *Definition of communication modes.*

Port	Transmission rate	Data bit	Stop bit	Parity check bit
RS-232	19200Baud	8-bit	one-bit	no

Table 2.2: *Formal description of the command framework.*

Instruction frame format	Length (bytes)	Instructions
Synchronization feature	1	0 FFH
talk	1	RS-232 communication time 00 h
mandate	1	Read the obtained 60 hours
Parametric length	1	00H
parameter	1	00H
Checksum	1	The remaining bytes without synchronized characters have a cumulative sum of 256 modules

Table 2.3: *Format description of data frames.*

Length of Command Frame format (bytes)	Length (bytes)	Instructions
Synchronization feature	1	0 FFH
Data length	1	09H
profile	1	00H
Checksum	1	The remaining bytes without synchronized characters have a cumulative sum of 256 modules

Table 2.4: *Formal description of the data area.*

Running parameter	Length (bytes)	Instructions
The amount of gas pedal movement	2	First low, then high
Brake pedal distance	2	First low, then high
Clutch travel	2	First low, then high
Steering Angle	2	First low, then high
Gear position	1	First low, then high
Checksum	1	The remaining bytes without synchronized characters have a cumulative sum of 256 modules

2.2.2. Communication with the Lower Computer. The lower computer communicates with the PC through the RS-232 interface. 89S52 built-in UART interface to achieve serial communication; the TXD needle is used to transmit data; The RXD needle is used to receive data. Since TXD and RXD pin adopt TTL level, RS-232 communication cannot be carried out, so the system chooses Maxim MAX232 to realize the switchover between the TTL level and the RS-232 level. This paper introduces an intelligent measurement system based on C language, which uses an interrupt service module to realize data sending and receiving in serial communication [8]. The flow chart of the main control program of the control system based on a single-chip microcomputer is shown in Figure 2.3. The implementation method of the serial interrupt service subroutine is shown in Figure 2.4.

2.3. Communication of the upper computer. PC communication software is based on VisualC++6.0 under Windows, and visual simulation is based on VegaAPI to call the rendering thread to complete. The PC's communication software is written using Windows API programming language. The communication requests received by the computer are usually asynchronous [9]. After receiving the serial communication

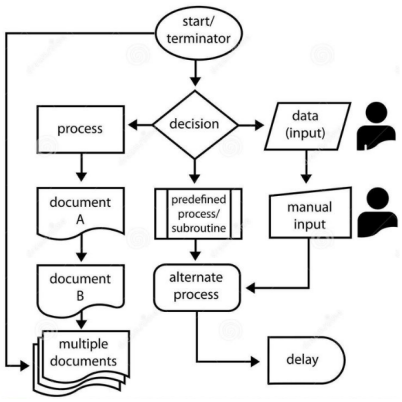

Fig. 2.3: . *Flow chart of the main control program of the lower computer.*

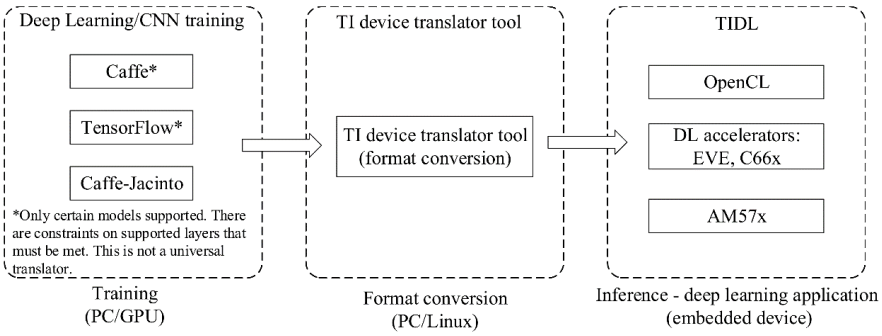

Fig. 2.4: *Flow chart of the traversing terminal service subroutine.*

request, the system only interacts with the communication buffer and does not generate the corresponding information to inform the user of the processing. When the user process needs to check its communication status periodically and actively access its communication buffer. Otherwise, requests for serial communication cannot be responded to quickly, resulting in a communication error that overflows the buffer. In addition, if an error occurs in the communication and is not detected, it will lead to a long pause in the communication process. The multithreading method is adopted in the design of the communication module to overcome the above problems and ensure the real-time performance of the system [10]. It realizes the readout of serial information through periodic queries. When the second layer communication thread detects a communication request, it sends a customized message to call the corresponding message processing function to read the traffic operation data. The serial communication between host computers is realized using multi-thread technology, and the concrete realization method is given. The serial communication flow of the host computer based on multithreading is shown in Figure 2.5.

3. The social force model of cars in emergencies.

3.1. Self-drive. Self-driving force G_a refers to a kind of social force automatically generated by subject a to achieve the desired purpose of driving in the emergency stage. Formula (3.1) is established:

$$G_a = \frac{M_a \left[\delta_a(t) - v_a(t)\right]}{\Delta t_a}$$

$v_a(t)$ is the speed and direction of the primary vehicle a in km/h.Δt_a is the adjustment time of the primary vehicle a in seconds. M_a is the equivalent weight of the primary vehicle a in kg.$\delta_a(t)$ is the expected speed

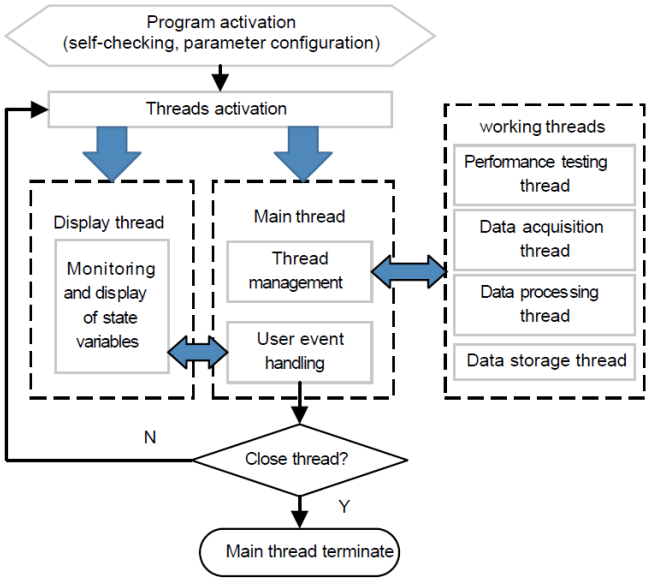

Fig. 2.5: *Flow chart of host computer serial communication based on multithreading.*

correction function (unit km/h) reflecting the environmental factors of driving behavior such as herd psychology and driving intention.

3.1.1. Expected speed correction function. When the leading car a realizes the driving goal, it will often adopt the driving mode conducive to its goal, but it will also be affected by the driving route of the surrounding vehicles [11]. It presents a kind of herd mentality. Therefore, the expected speed correction equation (3.2) is constructed to describe the driving goal and group mentality of car owner A:

$$\delta_a(t) = \lambda_a v_m(t) \left[\gamma_a \frac{v_{a+1}(t)}{|v_{a+1}(t)|}\right] \{\zeta_1, \zeta_2; \zeta_3\}$$

where λ_a is the correction of the leading car a. The positive factor of the school is affected by the surrounding traffic conditions. $v_m(t)$ is the current highway speed limit in km/h. $v_{a+1}(t)$ is the speed and amplitude of the vehicle in front at time t in km/h.γ_a is the conformity factor of vehicle a, which reflects the steering behavior of the vehicle [12]. Where ζ_1 is the unit vector used when turning left $(1/\sqrt{2}, 1/\sqrt{2})$ to reverse the cutting phase, and ζ_2 is the unit vector used when turning right to reverse the cutting phase $(1/\sqrt{2}, -1/\sqrt{2})$.$\zeta_3$ is a unit vector with a direction of $(1, 0)$ when turning to cut.

3.1.2. Equivalent mass. However, due to the driver's driving habits, methods, and other factors. Even in the same situation, drivers with different driving styles and habits will show different driving behaviors [13]. The power emitted in the same type of car will also significantly differ. Therefore, "equivalent mass" describes the driver and vehicle type based on a comprehensive driving style analysis for vehicle performance differences and other factors. Its expression is shown in formula (3.3):

$$M_a = M_a\left(m_a, C_a, S_a\right) = \frac{m_a\left(1 + S_a\right)}{C_a}$$

m_a is the weight of the primary vehicle a in kilograms. C_a is the type of the primary vehicle a, which is derived according to the type of vehicle. S_a is the driver type of the primary vehicle a based on the driving mode.

3.2. Repulsive forces between cars. When the vehicle a drives to the emergency section, in order to prevent conflict, the vehicle a coordinates with the rear vehicles in the same lane and the front and rear vehicles

in the target lane. The repulsive force is used to characterize the process of vehicle-vehicle collaboration [14]. It is divided into repulsive force $G_{a-1\to a}$ between a and the exact route vehicle | and repulsive force $G_{j\to a}$ between a and the destination line vehicle.

3.2.1. Original repulsive force. When there is an emergency in front of the primary vehicle a to prevent A secondary traffic accident, the car behind the same line will exert a repulsive force on the primary vehicle a. The formula is as follows (3.4):

$$G_{a-1\to a} = \begin{cases} \varphi_a \exp\left(\frac{\eta_a}{|f_{a-1,a}|}\right) \frac{f_{a-1,a}}{|f_{a-1,a}|}, |f_{a-1,a}| \le \eta_a \\ 0, |f_{a-1,a}| > \eta_a \end{cases}$$

φ_a is measured in N. It is the repulsive force of the leading car a when it is driving in the same road. η_a, in m, is the influence range of the repulsive force generated by the cars behind in the same lane on the central station a.$f_{a-1,a}$ is the vector between the car $a-1$ on the same line and the leading car a. It is measured in m, and its size is the distance between the middle points of two cars.

3.2.2. Road repulsion force. In the event of an emergency at the front, when the master station a is forced to change lanes, both the vehicles in front of and behind it in the target lane will exert A repulsive force on the master Station car a. The equation (3.5) is as follows:

$$G_{j\to a} = \begin{cases} \sigma_a \exp\left(\frac{\phi_a}{|f_{j,a}|}\right) \frac{f_{j,a}}{|f_{j,a}|}, |f_{j,a}| \le \phi_a \\ 0, |f_{j,a}| > \phi_a \end{cases}$$

| σ_a is measured in N. It is the repulsive force exerted by the primary car a on the front and behind cars in the target lane. ϕ_a in m, the leading car a is affected by the repulsive force of the car in the target lane. $f_{j,a}$ is the vector between the vehicle j and the primary vehicle a. It is measured in m and its size is the distance between two vehicles.

3.3. Repulsive force of vehicles in the emergency area. The primary vehicle a traveling in that position is subjected to the rejection of a sudden obstacle P to prevent a collision with a space object in an emergency. The equation (3.6) is as follows:

$$G_{P\to a} = \begin{cases} \omega_a \exp\left(\frac{\pi_a}{|f_{P,a}|}\right) \frac{f_{P,a}}{|f_{P,a}|}, |f_{P,a}| \le \pi_a \\ 0, |f_{P,a}| > \pi_a \end{cases}$$

ω_a is the repulsive force of a sudden obstacle P concerning the primary vehicle a. It's denoted by N. π_a is m for the area affected by the repulsive force of a burst barrier P.$f_{P,a}$ is a vector from the sudden occurrence of an obstacle P to the primary vehicle a, the size of which is the distance between the middle points of two vehicles in m.

3.4. The prescribed force of road alignment on motor vehicles. The car should maintain a distance from the surrounding rail when it is traveling to prevent deviation from the driving route [15]. As cars get closer, the tracks become more and more restrictive.

$$G_{M\to a} = Z_M \left| \frac{R}{2} - y_a \right| g$$

Z_M is the law force correction factor. R is the width of the lane in m.y_a is the distance from the center of the primary vehicle a to the lane represented by m. Where g is the buoyant force of the lane, the tangential turn to the left is $(0,-1)$, and the turn to the right is tangential $(0,1)$.

4. Performance verification. (1) The output of the multi-vehicle collaborative obstacle avoidance control algorithm is consistent with the actual measured value, and the multi-vehicle collaborative obstacle avoidance control algorithm can ensure that the vehicle can effectively avoid the obstacles that suddenly appear in front of it when it is driving. (2) The short-time memory method prediction results are close to the observed

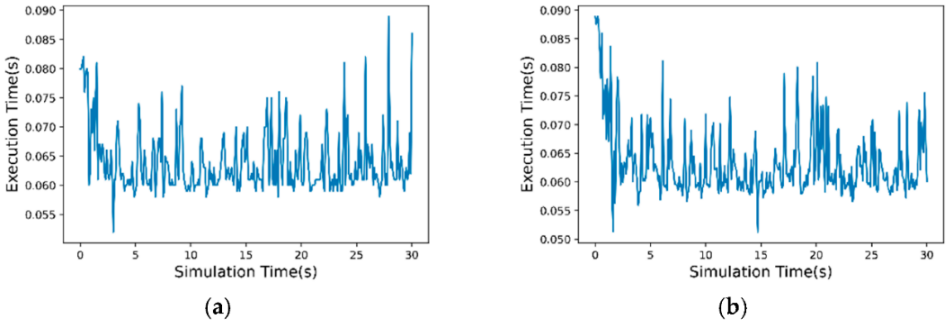

Fig. 4.1: *Performance of vehicle cooperative obstacle avoidance control strategy and lane-changing prediction model based on extended short-term memory algorithm in lane changing.*

Table 4.1: *Quantitative evaluation of vehicle cooperative obstacle avoidance control strategy and lane change prediction model based on extended short-term memory algorithm.*

Index		MSE	RMSE	MAE	RMSPE
Vehicle cooperative obstacle avoidance control	Longitudinal displacement	0.195	0.450	0.322	0.007
	Lateral displacement	0.053	0.235	0.060	0.004
	Longitudinal velocity	0.021	0.146	0.074	0.043
	Lateral velocity	0.005	0.077	0.033	0.141
Long short-term memory algorithm	Longitudinal displacement	25.106	5.114	3.466	0.086
	Lateral displacement	0.030	0.177	0.115	0.003
	Longitudinal velocity	9.530	3.151	2.053	0.916
	Lateral velocity	0.500	0.722	0.360	1.328

values. However, the short-time memory method's prediction model is still slow when encountering sudden accidents and cannot avoid sudden obstacles [16]. It can not effectively decide on vehicle direction changes during traffic accidents. This project intends to evaluate this method from four aspects quantitatively to verify the effectiveness of this method compared with the long-term memory path planning method: mean square error, root mean square error, mean absolute error, mean absolute error and mean absolute error [17]. It can be seen from the table that the calculation accuracy of the vehicle collaborative collision avoidance method is much lower than the actual measurement value, which indicates the superiority of the method.

5. Conclusion. A human-computer interaction system for in-loop simulation of man-vehicle-road systems is established using single-chip microcomputer technology and computer serial communication technology. The system uses a distributed up-and-down machine architecture, and the up-and-down devices communicate point-to-point through an RS-232 serial port. This project proposes a rapid direction change and collision avoidance method based on lane change technology. It is found that this method can better reflect the interaction between the car and the surrounding vehicles. Compared with the route planning method based solely on short and long-term memory, this project focuses on the traffic congestion caused by uncertain factors such as traffic accidents in the traffic environment. It enables driverless cars to change lanes and evade autonomously. This method uses multi-thread and multi-level query modes. The design ideas adopted are also relevant to other human-computer interactive environments.

REFERENCES

[1] Zapiee, M. K., Mohana, D., Balasingam, S., & Panessai, I. Y. (2022). Disaster Sites Roaming Smart Car with Hand Gesture Controller. International Journal of Recent Technology and Applied Science (IJORTAS), 4(1), 31-43.

[2] Dhiran, M. (2021). Role of Human Computer Interaction. Turkish Journal of Computer and Mathematics Education (TURCOMAT), 12(13), 159-163.
[3] Yang, J. J., Chen, Y. M., Xing, S. S., & Qiu, R. Z. (2023). A comfort evaluation method based on an intelligent car cockpit. Human Factors and Ergonomics in Manufacturing & Service Industries, 33(1), 104-117.
[4] Chen, X., Cao, M., Wei, H., Shang, Z., & Zhang, L. (2021). Patient emotion recognition in human computer interaction system based on machine learning method and interactive design theory. Journal of Medical Imaging and Health Informatics, 11(2), 307-312.
[5] Detjen, H., Faltaous, S., Pfleging, B., Geisler, S., & Schneegass, S. (2021). How to increase automated vehicles' acceptance through in-vehicle interaction design: A review. International Journal of Human–Computer Interaction, 37(4), 308-330.
[6] Barricelli, B. R., & Fogli, D. (2024). Digital twins in human-computer interaction: A systematic review. International Journal of Human–Computer Interaction, 40(2), 79-97.
[7] Zhang, R., Jiang, C., Wu, S., Zhou, Q., Jing, X., & Mu, J. (2022). Wi-Fi sensing for joint gesture recognition and human identification from few samples in human-computer interaction. IEEE Journal on Selected Areas in Communications, 40(7), 2193-2205.
[8] Chen, X., Xu, L., Cao, M., Zhang, T., Shang, Z., & Zhang, L. (2021). Design and implementation of human-computer interaction systems based on transfer support vector machine and EEG signal for depression patients' emotion recognition. Journal of Medical Imaging and Health Informatics, 11(3), 948-954.
[9] Karahasanović, A., & Culén, A. L. (2023). Project-based learning in human–computer interaction: a service-dominant logic approach. Interactive Technology and Smart Education, 20(1), 122-141.
[10] Liu, R., Liu, Q., Zhu, H., & Cao, H. (2022). Multistage Deep Transfer Learning for EmIoT-Enabled Human–Computer Interaction. IEEE Internet of Things Journal, 9(16), 15128-15137.
[11] Xu, H. (2022). Intelligent automobile auxiliary propagation system based on speech recognition and AI driven feature extraction techniques. International Journal of Speech Technology, 25(4), 893-905.
[12] Schomakers, E. M., Lidynia, C., & Ziefle, M. (2022). The role of privacy in the acceptance of smart technologies: Applying the privacy calculus to technology acceptance. International Journal of Human–Computer Interaction, 38(13), 1276-1289.
[13] Jia, L., Zhou, X., & Xue, C. (2022). Non-trajectory-based gesture recognition in human-computer interaction based on hand skeleton data. Multimedia Tools and Applications, 81(15), 20509-20539.
[14] Diederich, S., Brendel, A. B., Morana, S., & Kolbe, L. (2022). On the design of and interaction with conversational agents: An organizing and assessing review of human-computer interaction research. Journal of the Association for Information Systems, 23(1), 96-138.
[15] Zhu, Y., Tang, G., Liu, W., & Qi, R. (2022). How post 90's gesture interact with automobile skylight. International Journal of Human–Computer Interaction, 38(5), 395-405.
[16] Sevcenko, N., Appel, T., Ninaus, M., Moeller, K., & Gerjets, P. (2023). Theory-based approach for assessing cognitive load during time-critical resource-managing human–computer interactions: an eye-tracking study. Journal on Multimodal User Interfaces, 17(1), 1-19.
[17] Paul, S., Yuan, L., Jain, H. K., Robert Jr, L. P., Spohrer, J., & Lifshitz-Assaf, H. (2022). Intelligence augmentation: Human factors in AI and future of work. AIS Transactions on Human-Computer Interaction, 14(3), 426-445.

Edited by: Hailong Li
Special issue on: Deep Learning in Healthcare
Received: Mar 1, 2024
Accepted: Apr 14, 2024